

Electronic Supplementary Information

Direct Growth of Carbon Nanotubes on Ni/TiO₂ as Next Generation Catalysts for Photoreduction of CO₂ to Methane by Water under Visible Light Irradiation

Wee-Jun Ong,^a Meei Mei Gui,^a Siang-Piao Chai^{*a} and Abdul Rahman Mohamed^b

^a *Low Carbon Economy (LCE) Group, Chemical Engineering Discipline, School of Engineering, Monash University, Jalan Lagoon Selatan, Bandar Sunway, 46150, Selangor, Malaysia.*

^b *Low Carbon Economy (LCE) Group, School of Chemical Engineering, Universiti Sains Malaysia, Engineering Campus, Seri Ampangan, 14300 Nibong Tebal, Pulau Pinang, Malaysia.*

* Corresponding author.

Tel: +603-5514 6234; Fax: +603-5514 6207

E-mail address: chai.siang.piao@monash.edu

EXPERIMENTAL METHODS

Chemicals. All chemicals were reagent-grade and deionized water was used in the whole experiment. Nickel (II) nitrate hexahydrate, $\text{Ni}(\text{NO}_3)_2 \cdot 6\text{H}_2\text{O}$ (Sigma Aldrich Malaysia >98% purity) was used as the dopant metal salt. Pure anatase TiO_2 nanopowder (Sigma Aldrich Malaysia >98% purity) was used as the support as well as serve as the semiconductor in photocatalysis. Sodium hydroxide, NaOH (Merck, 99% purity) was used as the precipitating agent. Glycerol (Fisher Scientific, 95% purity) was served as the complexing agent for nickel. The use of glycerol favours the formation of small Ni particles prohibiting the aggregation of metal particles. All chemicals were used as received without any further purification for all studies.

Synthesis of Ni/TiO₂. Ni-doped TiO_2 catalysts were prepared *via* co-precipitation method using NaOH as precipitating agent. The calculated amount of $\text{Ni}(\text{NO}_3)_2 \cdot 6\text{H}_2\text{O}$ was dissolved in deionized water followed by the addition of glycerol which favors the formation of small Ni particles prohibiting aggregation of Ni particles. The nickel-glycerol complex was precipitated on TiO_2 nanoparticles by adding NaOH dropwise into the suspension until a final pH of 8.5 was achieved. The solution was continuously stirred for 2 h prior to filtering and the precipitate was dried at 105 °C. The dried photocatalyst was then calcined in air at 550 °C for 5 h. The loading of Ni into the TiO_2 nanoparticles was 10 wt%. The resultant Ni-incorporated TiO_2 catalyst was then used for the synthesis of novel CNT@Ni/TiO₂ nanostructured composite *via* chemical vapor deposition (CVD) growth of CNTs onto the Ni/TiO₂ particles.

Synthesis of CNT@Ni/TiO₂. Synthesis of CNTs was conducted at 750 °C for 2 h under the gas flow of CH_4 and H_2/Ar . The Ni-supported TiO_2 nanocomposite was placed in a quartz boat at the

middle part of the reactor which was mounted in an electrical furnace. The reaction temperature was increased gradually to the CVD temperature at 750 °C in 3% H₂/Ar inert gas flow rate of 40 ml/min. Ar was flowed into the horizontal quartz reactor to prevent the oxidation of metal catalysts while raising the temperature. Meanwhile, the 3% H₂ under an H₂/Ar atmosphere was used to reduce the nickel oxide (Ni²⁺) to nickel metal (Ni). When the catalyst was heated up to the CVD temperature, the flow of CH₄ (40 ml/min) was started and flowed simultaneously with 40 ml/min of 3% H₂/Ar. The flow of gases was controlled using respective mass flow controllers supplied by Brooks Instrument. The duration of CVD process was fixed to be 2 h. At the end of reaction process, the flow of CH₄ was stopped. The inert gas was continuously flowing to reduce the sample temperature to the room temperature.

Materials Characterization. The surface morphology and structure of the CNTs grown from the catalyst surface were analyzed by field emission scanning electron microscopy (FE-SEM) (Hitachi SU8010). High resolution transmission electron microscopy (HR-TEM) images were taken with a JEOL JEM-2100F microscope operated at 200 kV. The TEM sample was created by depositing a drop of diluted suspensions in ethanol on a lacey-film-coated copper grid. The crystalline phase of CNT@Ni/TiO₂ photocatalysts was identified based on the 2θ values from powder X-ray diffraction (XRD) (D8 Advance X-Ray Diffractometer – Bruker AXS) using Ni-filtered Cu K α radiation ($\lambda = 0.154056$ nm) as the X-ray source operated at 40 kV. UV-Vis absorbance spectra were obtained for the photocatalysts using a UV-Vis spectrophotometer (Agilent, Cary 100) equipped with an integrated sphere. The absorbance spectra of the photocatalysts were analyzed under ambient temperature in the wavelength range of 300–800 nm. The band gap energies of the photocatalysts were determined from the Kubelka-Munk function, $F(R)$ and the extrapolation of Tauc plot which is a plot of $[F(R)\cdot h\nu]^{1/2}$ versus $h\nu$. The

thermal stability of CNT@Ni/TiO₂ nanocomposite was determined from the weight loss measurements by heating the samples from ambient temperature to 900 °C with an air flow rate of 40 ml/min and a heating rate of 10 °C/min using thermogravimetric analysis (TGA) system (TA Q-50). Raman spectra were recorded at room temperature using Renishaw inVia Raman Microscope in the back-scattering geometry with Ar⁺ laser excitation at 514 nm in the range of 100–3000 cm⁻¹.

Photocatalytic experiments. For the CO₂ photocatalytic reaction, high purity of CO₂ was flowed through a water bubbler to produce a mixture of CO₂ and water vapor at atmospheric pressure. The flow rate of CO₂ was fixed at 6 ml/min and then it bubbled through the deionized water in a conical flask on the heating mantle at 50 °C. The percentage humidity of wet CO₂ gas was found to be 60%. Before the irradiation of visible light, wet CO₂ was first flowed through the quartz tube loaded with the coated photocatalysts (TiO₂, Ni/TiO₂ or CNT@Ni/TiO₂) on glass rods for 60 min to ensure that the air was totally eliminated and also to achieve complete adsorption of gas molecules. After 60 min of purging, the visible light was turned on and the yield of CH₄ produced as a function of irradiation time was determined. The reactant gas was then in contact with photocatalysts under the illumination of low-power 75 W visible daylight lamp to provide a full spectrum emission without any filter to simulate the sunlight source for a total of 10 h. The average intensity of the visible light was 720 Lux using a lumen meter. The distance apart between the visible light source and the photoreactor was fixed to be 6 cm. The feed gas stream and the product gases from the photoreactor were analyzed by an Agilent 7890A gas chromatography (GC) through an automated gas valve using helium as the carrier gas to determine the CH₄ product yield (as shown in Equation 1) from the photocatalytic reaction. The GC was equipped with flame ionization detector (FID). Meanwhile, for the control experiment, a

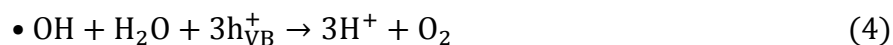
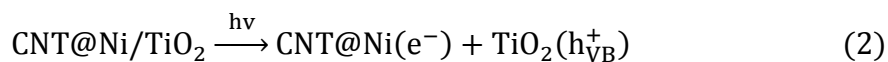
blank experiment was conducted to ensure that the CH₄ product formed was due to the photoreduction of CO₂ in order to eliminate the surrounding interference. The control experiment was performed by introducing the wet CO₂ through the CNT@Ni/TiO₂ nanocomposites in the dark condition (without irradiation of light source). The photocatalytic experiments were performed in duplicate under the same reaction conditions to ensure the reproducibility in the catalyst activity whereby consistent results with significant less variations were obtained.

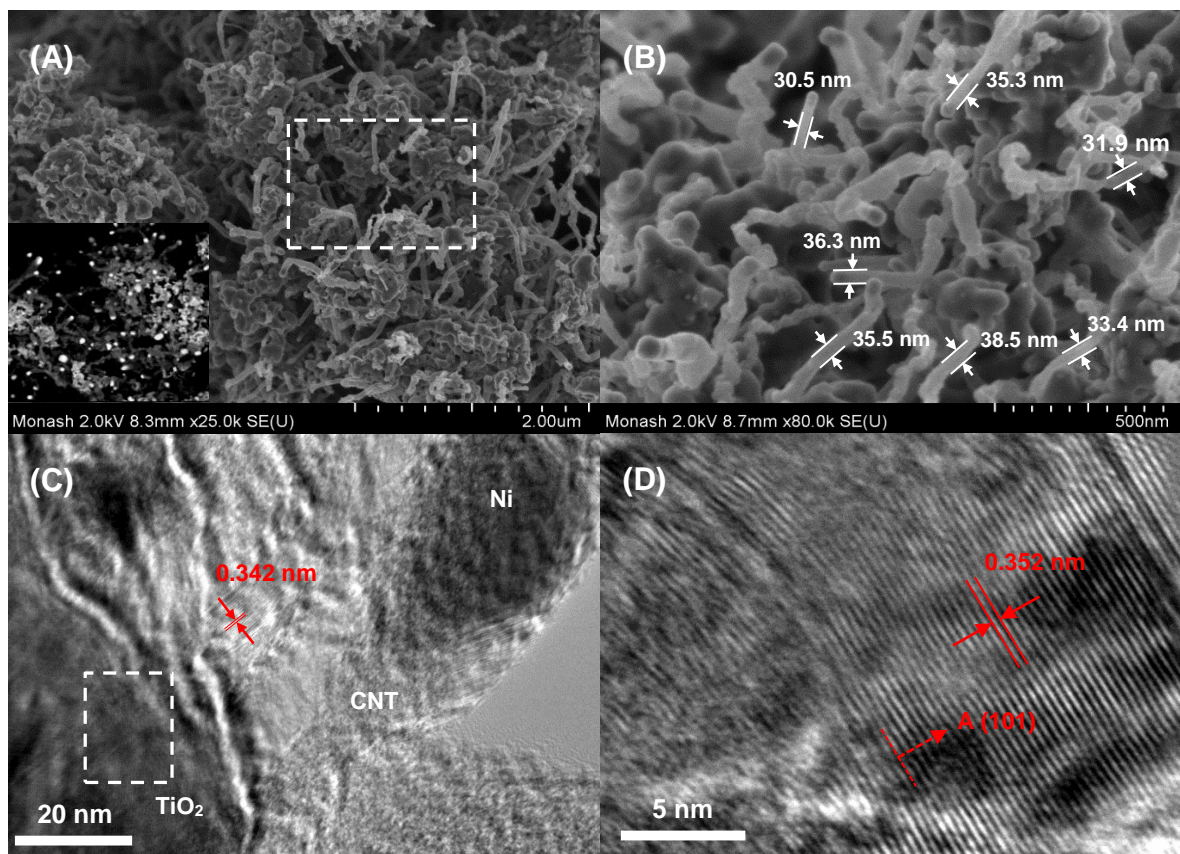
$$\text{Yield } (\mu\text{mol CH}_4 \text{ g}^{-1} \text{ catalyst}^{-1} \text{ h}^{-1}) = \frac{(C_{\text{final,CH}_4} - C_{\text{initial,CH}_4}) \times \text{volumetric flow rate of product gas}}{\text{mass of photocatalysts used}} \quad (1)$$

Reaction Mechanism for the Enhancement of the Photocatalytic Activity of TiO₂ by CNTs

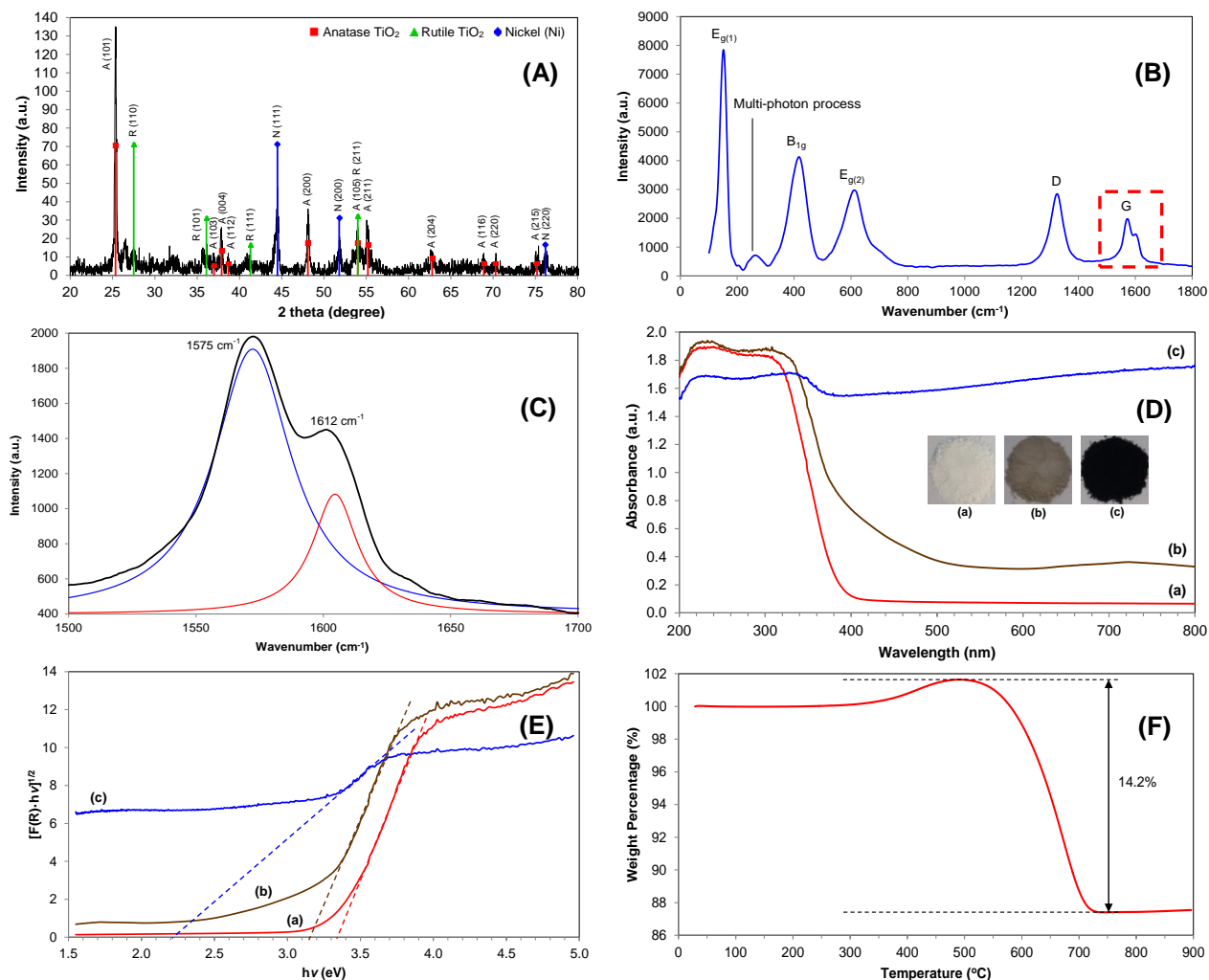
Under illumination of visible light, TiO₂ absorbs the irradiation and excites the electrons from the VB to the CB of TiO₂ (Eq. 2). The excited electrons can be shuttled freely along the conducting network of CNTs acting as electron reservoir allowing charge separation, stabilization and hindered recombination (Eq. 2). The electrons, that have not recombined would be stored in the CNTs and Ni (lower Fermi level than that of TiO₂), react with CO₂ to trigger the formation of a very negative superoxide radical ion ($\bullet \text{CO}_2^-$) (Eq. 6). Simultaneously, the longer-lived positively charged holes (h^+) at the VB edge of TiO₂ react with adsorbed water molecules to produce hydroxyl radical ($\bullet \text{OH}$) and subsequently H^+ and O_2 (Eqs. 3–4). The interaction of H^+ ions with the excited electrons leads to the formation of $\bullet \text{H}$ radicals (Eq. 5). Then the incipient $\bullet \text{CO}_2^-$ radicals and $\bullet \text{H}$ radicals react with each other to produce CO (Eq. 7). Carbon radicals ($\bullet \text{C}$) were formed from CO through successive reactions (Eqs. 8–9) followed by a series of $\bullet \text{CH}$, $\bullet \text{CH}_2$ and $\bullet \text{CH}_3$ radicals (Eqs. 10–12). Lastly, the $\bullet \text{CH}_3$ radicals react with protons to produce

CH₄ (Eq. 13). The overall chemical reaction for the photoreduction of CO₂ to CH₄ is shown in Eq. 14 where a total of eight electrons are required for the reaction to proceed. Therefore, these radical groups are responsible for the photoreduction of CO₂ to CH₄. The following reaction scheme (Eqs. 2–14) was proposed when CO₂, H₂O and CNT@Ni/TiO₂ photocatalysts were in contact with visible light source.

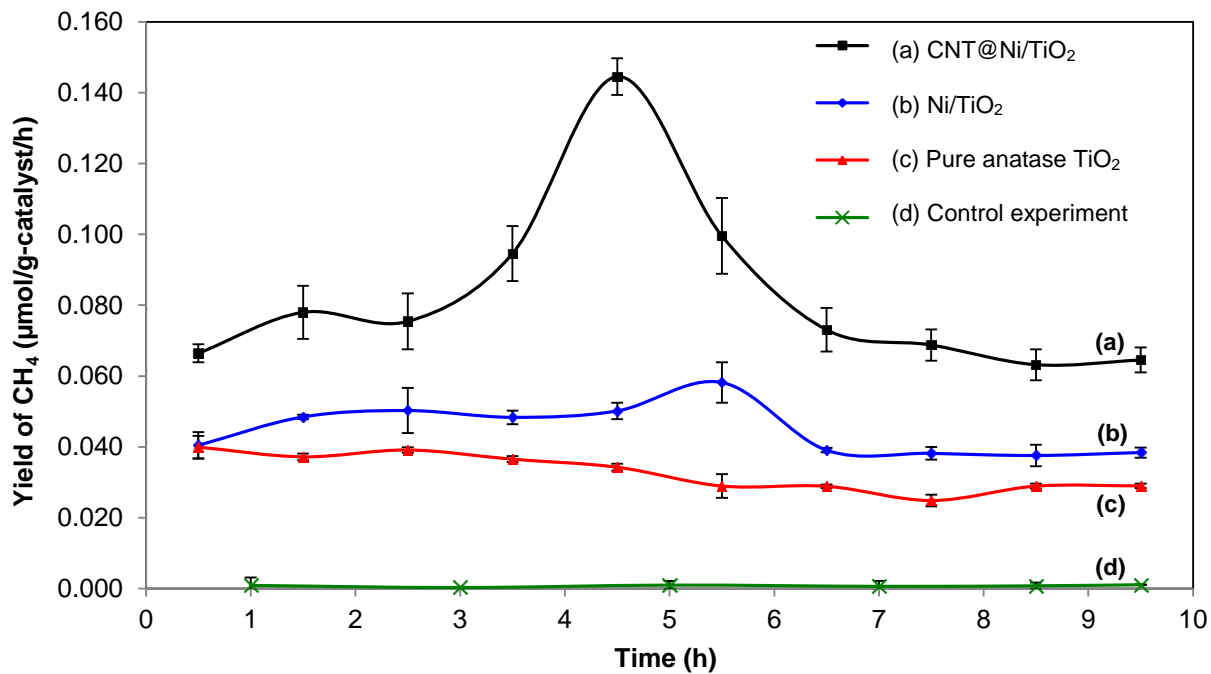




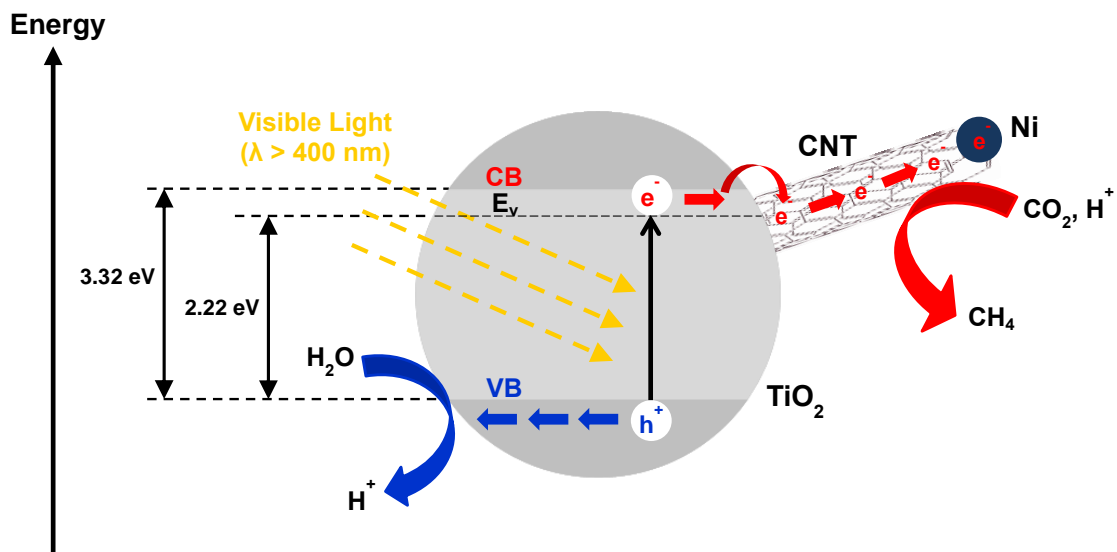
Enlarged Fig. 1 Electron microscopy of the CNT@Ni/TiO₂ nanocomposites: (A) Low magnification of FE-SEM (inset is a back-scattered electron imaging), (B) High magnification of FE-SEM, (C) HR-TEM image and (D) Enlarged HR-TEM lattice spacings with dominant crystal facet of anatase, A (101).



Enlarged Fig. 2 (A) XRD pattern of CNT@Ni/TiO₂. A denotes anatase TiO₂, R denotes rutile TiO₂, N denotes nickel. (B) Raman spectrum of CNT@Ni/TiO₂. (C) Fitting curve of G-band of graphite with Lorentzian equation. (D) UV-Vis spectra of (a) pure anatase TiO₂, (b) Ni/TiO₂ and (c) CNT@Ni/TiO₂ (inset shows the colors of photocatalysts (a), (b) and (c)). (E) Plot of transformed KM function $[F(R) \cdot hv]^{1/2}$ vs. hv for (a) pure anatase TiO₂, (b) Ni/TiO₂ and (c) CNT@Ni/TiO₂. (F) TGA curve of CNT@Ni/TiO₂.



Enlarged Fig. 3 Time dependence on the production rate of CH₄ over (a) CNT@Ni/TiO₂, (b) Ni/TiO₂, (c) pure anatase TiO₂ and (d) control experiment using CNT@Ni/TiO₂ without light irradiation.



Enlarged Scheme 1 Schematic illustration of the charge transfer for photoreduction of CO₂ with H₂O using CNT@Ni/TiO₂ nanocomposites under visible light irradiation with the introduction of new energy level, E_v.